Supplementary information to: A quasi-atomic model of human Adenovirus type 5 capsid

By: Fabry, Rosa-Calatrava, Conway, Zubieta, Cusack, Ruigrok and Schoehn.

Methods

Fitting the atomic structures of hexon and penton base into the EM map.

The atomic structures of the Ad5 hexon (residues 5-946, full length of hexon is 951 residues, Rux and Burnett, 2000; PDB number 1RUX) and that of the Ad2 penton base (residues 52-567, 1-48 are missing, 49-51 disordered, 299-372 disordered; Zubieta et al. 2005, PDB number 1X9P; structure of penton base plus a 20 amino acid N-terminal peptide, PDB number 1X9T) were fitted into the EM model for wt Ad5.

Penton base. The atomic structure the penton base was placed manually into one penton base using the program "O" (Jones et al, 1991). Using SPIDER (Frank et al, 1996), the atomic model of the penton base was filtered to a resolution of 11 Å in order to create a binary mask (value of 1 for everything inside the penton base and 0 for everything outside). This mask was then enlarged by a factor of 1.6 in order to be sure that any loops that are visible in the EM model of the penton base but invisible in the atomic model (due to disorder) are included for the positioning process. The EM map was the multiplied by the 11 Å binary mask. The mask contained the density of the penton base but also some density from neighbouring molecules (such as neighbouring hexons or minor proteins). The position of the atomic model of the penton base was then optimised into the isolated penton from the EM map with SITUS (Wriggers and Birmanns 2001). The 11 other pentons were generated using icosahedral symmetry and the quality of the fit was then checked manually using "O".

Hexons. The atomic structures of the hexon was placed manually into the four hexons that make up the Asymmetric Unit (AU) using the program "O" (Jones et al, 1991). URO (Navaza et al, 2002) was used to generate a preliminary quasi-atomic model of the entire hexon shell of the virus

using the 4 manually positioned atomic structures of hexon in the AU. For this first model, a mask was made using SPIDER in order to exclude as much density as possible that did not belong to the hexon trimers. This mask was then used to restart URO and to find the final position of the four hexons in the asymmetric unit. The quality of the final fit is given by a correlation coefficient of 94.4 % and crystallographic Rfactor of 26.7 %. We also checked the quality of the fit visually and with the softwares mapman and mama (Upsala Software Factory). For the 240 hexons, an averaged value of 0.9 % of the atoms from the X-ray structure falls outside the EM map (hexon 1 : 0.83%, hexon 2: 0.86 % hexon 3 : 0.92; hexon 4: 0.96 %. These difference are not significant enough to say that one hexon fit is better then the other. In the case of the penton base this value is 1.82% which means that this fit is of slightly lower quality. The scale of the EM map was also tested using URO and this agreed with the value obtained using TMV as a magnification standard (i.e. 2.45 Å/pixel). From the optimised positions of the 4 hexons in the asymmetric unit plus the penton, the quasi-atomic model of the whole capsid was built using 532 icosahedral symmetry.

Generation of EM difference maps

The difference maps were generated by using the quasi atomic model of the capsid. This model was Fourier filtered to the same resolution as the EM maps. We then created a binary mask (value of 0 for everything inside the capsid and 1 for everything outside) that included the right molecular weight of the capsid. Then, the different EM maps were multiplied by their corresponding binary masks to generate the difference maps.

Contacts between capsomers.

Protein contacts between capsomers were defined as any pair with atoms closer than 5 Å. This analysis was done by visual inspection of the EM density and the quasi-atomic model using "O" and verified using Contact v5.0 from the CCP4 suite.

Determination of the resolution for the EM reconstructions of wt Ad5 (A), *sift* Ad5 pIX° (B) and *muft* Ad5 pIX° (C).

The resolution of the EM reconstructions structures was determined by Fourier Shell Correlation using a threshold value of 0.3 (Yang et al., 2003). The images used for the reconstructions were split into two halves in order to calculate two independent reconstructions. The Fourier shell correlations for these two reconstructions are indicated in Figure 1.

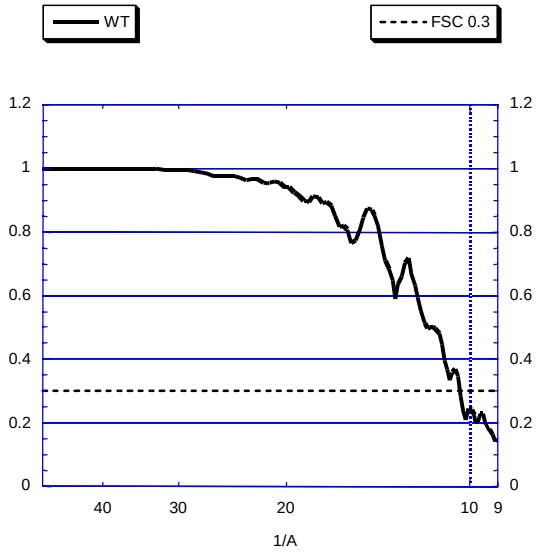

Figure 1A - The resolution of the wild type Ad5 EM reconstruction was estimated by Fourier shell correlation (FSC). The horizontal dashed line represents a conservative estimate where the power in the EM map falls to a FSC of 0.3. The estimated value for the resolution is 10.3 Å.

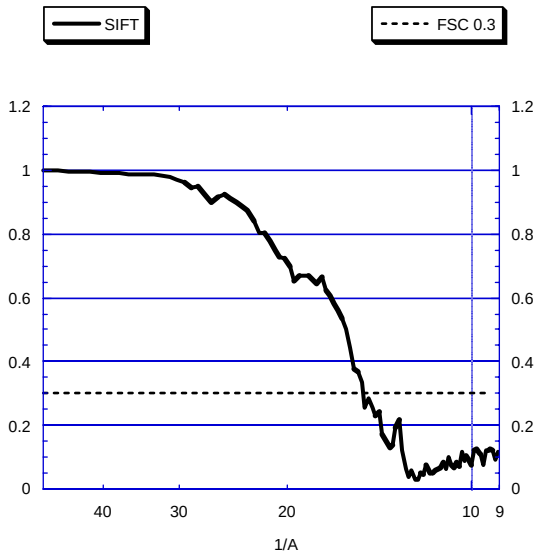

Figure 1B - Resolution of the *sift* Ad5 pIX° reconstruction. Estimated resolution: 15.0 Å.

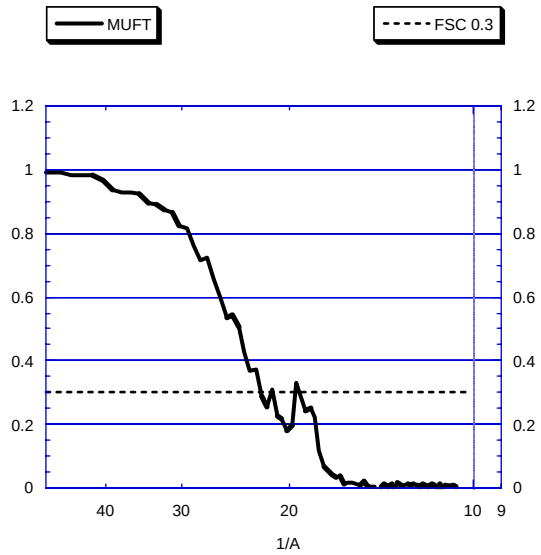

Figure 1C - Resolution of the *muft* Ad5 pIX° reconstruction. Estimated resolution 22.3 Å (the FSC curve crosses the 0.3 line also at 21.3 and 19.4 Å).

Biochemical evidence that most of protein IIIa in Ad5 pIX° virus and in Ad5 viruses mutated in the gene for pIX, is dissociated from virus after freezing/thawing.

The *sift* pIX mutant virus neither contained pIX, which was expected since the gene for this protein had been deleted, but also protein IIIa. We analysed stocks of wt, pIX° and other mutant Ad5 viruses that had short deletions in the gene for pIX (Ad5 pIX mutant Δ22-23 and mutant Δ26-28, described in Rosa-Calatrava et al., 2001). We analysed the same viruses on SDS-PAGE after pelleting them through a 20% glycerol cushion in order to remove viral proteins that have dissociated from the capsid (Figure 2). All viruses had been frozen/thawed a single time (so comparable with the *sift* pIX° virus sample used for the cryo-EM reconstruction). In all virus stocks the band for protein IIIa was much stronger than that for the fibre, in agreement with the fact that there are 60 IIIa molecules per virus particle compared with only 36 fibre monomers per virion. After the centrifugation step, only a small amount of the pIX° mutant virus was found in the pellet but much more of the other two mutant viruses. However, in the pellets of all mutant viruses, the ratio between the densities for fibre and protein IIIa had been inverted with a strong band for fibre and only a weak band for IIIa. This indicates that these viruses had lost a significant amount of their protein IIIa, probably through the freezing/thawing treatment. We were not able to obtain virus

preparations that had lost all protein IIIa. This may imply that some IIIa was retained in the pIX° virus that was analysed by cryo-EM. However, if the occupancy of IIIa was significantly lower than that of the other virus proteins, the cut-off values for the EM density would have resulted in elimination of the density for IIIa. Penton base protein and protein IIIa are also the first proteins that dissociate from wt Ad5 when incubated at elevated temperatures (Rexroad et al., 2003).

Figure 2; SDS Page analysis of wt and mutant Ad5 viruses, stock solutions and after pelleting the virus through a glycerol cushion. Numbers on the left indicate molecular weight markers whereas some of the viral proteins are indicated on the right.

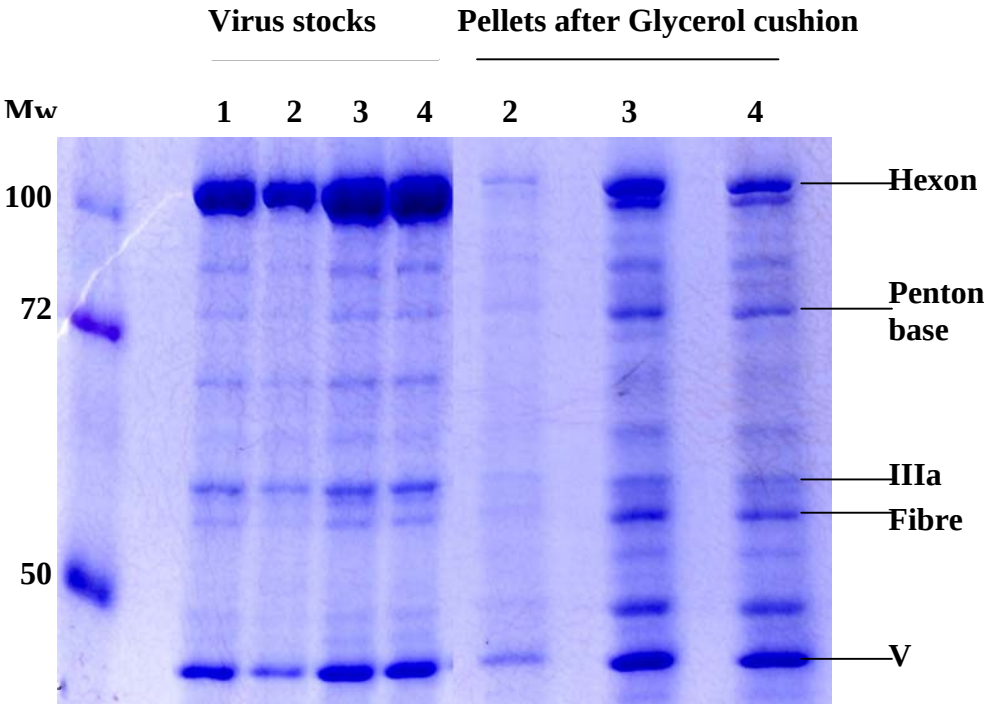

1 wt Ad5
2 Ad5 pIX°
3 Ad5 pIX mutant Δ22-23
4 Ad5 pIX mutant Δ26-28

References

Frank, J., Radermacher, M., Penczek, P., Zhu, J., Li, Y., Ladjadj, M. and Leith, A. (1996) SPIDER and WEB: processing and visualization of images in 3D electron microscopy and related fields. *J Struct Biol*, **116**, 190-199.

Jones, T.A., Zou, J.Y., Cowan, S.W. and Kjeldgaard. (1991) Improved methods for building protein models in electron density maps and the location of errors in these models. *Acta Crystallogr A*, **47 (Pt 2)**, 110-119.

Navaza, J., Lepault, J., Rey, F.A., Alvarez-Rua, C. and Borge, J. (2002) On the fitting of model electron densities into EM reconstructions: a reciprocal-space formulation. *Acta Crystallogr D Biol Crystallogr*, **58**, 1820-1825.

Rexroad, J;, Wiethoff, C.M., Green, A.P., Kierstead, T.D., Scott, M.O. and Middaugh, C.R. (2003). Structural stability of adenovirus type 5. *J Pharm Sci* **92**, 665-678.

Rosa-Calatrava, M., Grave, L., Puvion-Dutilleul, F., Chatton, B. and Kedinger, C. (2001). Functional analysis of adenovirus protein IX identifies domains involved in capsid stability, transcriptional activity and nuclear reorganisation. *J Virol* **75**, 7131-7141.

Rux, J.J. and Burnett, R.M. (2000) Type-specific epitope locations revealed by X-ray crystallographic study of adenovirus type 5 hexon. *Mol Ther*, **1**, 18-30.

Wriggers, W. and Birmanns, S. (2001) Using situs for flexible and rigid-body fitting of multiresolution single-molecule data. *J Struct Biol*, **133**, 193-202.

Yang, S., Yu, X., Galkin, V.E. and Egelman, E.H. (2003). Issues of resolution and polymorphism in single-particle reconstruction. *J. Struct. Biol*. **144**, 162-171.

Zubieta, C., Schoehn, G., Chroboczek, J. and Cusack, S. (2005) The structure of the human adenovirus 2 penton. *Mol Cell*, **17**, 121-135.